Modeling, Design and control of Planar parallel platform-based isolator mechanism

K V Varalakshmi, J Srinivas

Abstract

This paper proposes a motion isolation methodology by using a planar parallel linkage with two kinds of control schemes. Base excitations including the ground oscillations and resonance vibrations due to nearby equipment induce unexpected high end response at the instrument platforms. The concept of passive isolation is nowadays replaced by semi-active and active methods. This work proposes, the methodology of using a simple planar 3-RRR parallel mechanism having well known dynamic behaviour. Initially an excitation in the form of random base motion as translation is provided at the active joints and the corresponding transmitted displacements through the elastic links onto the mobile platform are reported. In the semi-active isolation approach an isolator having spring-damper element is considered and the effective isolation is obtained by tuning the spring and dashpot constants. In the active-isolation scheme, it is proposed to utilize the principle of active control, where the calculated motor torques are provided according to the instantaneous response obtained at the mobile platform. Effectiveness of the schemes is illustrated with a case study.

Keywords: Manipulator-dynamics, Isolation, Computed torque control, Planar mechanism, Base excitation.

1 Introduction

In precise instrumentation including atomic force microscopes, interferometers, optical measuring instruments and co-ordinate measuring machines, ofen a base isolator is employed to minimize the effects of ground noise in measurements. Such a kind of external disturbances need compensation by a suitable rejection mechanism. Various isolator mechanisms have been proposed in literature based on several parallel manipulator mechanisms. The very first such isolator was designed with Stewart-Gough platform possessing 6-degrees of freedom at mobile base. Later on, several such isolators were implemented with various spatial and planar mechanisms [1-3]. Multi-dimensional vibration isolation is principally classified as passive [4, 5], semi-active [6-8] and active vibration isolation [9, 10]. Passive vibration isolation relies on the use of materials like rubber, air cushion, mechanical spring, etc., but these materials have to produce supporting force of the load. Hence, the system's natural frequency cannot be very low. Therefore, passive vibration isolation is not effective for low or ultra-low frequency vibration. Semi-active

K V Varalakshmi
Department of Mechanical Engineering, NIT Rourkela, Odisha-769008, India, E-mail:kv.varalakshmi@gmail.com.

J Srinivas (Corresponding author)
Department of Mechanical Engineering, NIT Rourkela, Odisha-769008, India, E-mail:srin07@yahoo.co.in.

vibration isolation regulates damping force by controlling adjustable damping devices such as a magneto-rheological damper to suppress the harmonic peak, however the system's natural frequency continues to be not reduced and hence semi-active vibration isolation capability is limited. Instead of directly opposing a primary disturbance, semi-active vibration control is used to apply a secondary force, which counteracts the effects of the disturbance by altering the properties of the system, such as stiffness and damping [11]. Active vibration isolation is realized by the use of closed-loop calibration; this method is very flexible and effective for low-frequency vibration isolation and also, the reliability and robustness are also very low for this method. Yao et al. [12] studied the control of the vehicle suspension system with MR damper. Most of the semi-active isolation systems are on-off variety, some of the authors are introduced the skyhook control in semi-active vibration to improve the control strategy. When comparing to passive and semi-active isolation schemes the active isolation achieves better isolation with control techniques. Various control techniques [13-15] such as H^{∞}, μ-synthesis, robust nonlinear controllers were used for tracking control and active vibration control in both joint space and task space. Even though several studies were conducted by many authors on active isolation, they are far from perfect. Therefore, more attention is required for active isolation with different control strategies. In the present work, the vibration/motion isolation performance of the set-up based on 3-RRR parallel linkage is presented. Displacement transmissibility is estimated through semi-active and active isolation schemes through simulations. Active isolation with computed torque control (CTC) scheme is used for the effective performance of the isoaltion. A task space controller is developed to reduce the positional errors at the end-effector.

2 System Description and Modeling

A schematic of 3-RRR planar parallel platform-based isolator is shown in Fig. 1.

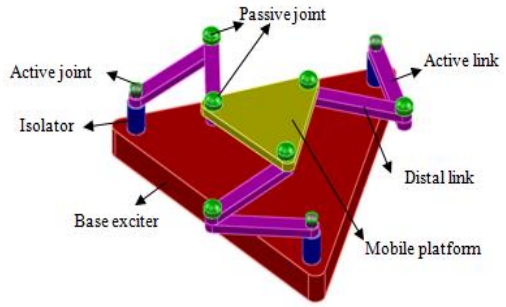

Figure 1: Plane motion- isolation system under consideration

The platform has planar motion at its output space. The mechanism consists of three identical branches connecting the base with mobile platform. Each branch has one active joint at the base and two passive joints connecting the active and distal links with mobile platform. In simple sense, a semi-active spring-damper system is initially considered at each active joint location. One has to either design the motion isolation at the base joints level or control the motion of each leg so that the base motion would not be transmitted to the mobile platform .

2.1 Modeling of Single axis isolator

In semi-active isolation the planar parallel mechanism is represented by the single DOF system at each active joint whose base is subjected to an excitation x_0. The displacement response x_1 at the mobile platform is measured based on governing motion equation of the system. Here, no external force directly applied to the mobile platform. The equations of motion for the single DOF isolation system consist of a linear spring in parallel with a passive damper as shown in Fig. 2 are given as:

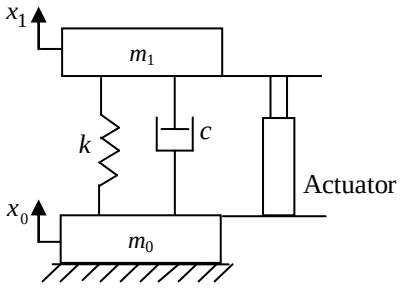

Figure 2: Semi-active control

$$m_0\ddot{x}_0 + c(\dot{x}_0 - \dot{x}_1) + k(x_0 - x_1) = F_d - F_a \quad (1a)$$

$$m_1\ddot{x}_1 + c(\dot{x}_1 - \dot{x}_0) + k(x_1 - x_0) = F_a \quad (1b)$$

where m_0 and m_1 are the mass of base and mobile platform respectively, k and c are the stiffness and damping of the isolator respectively. F_d and F_a are the input disturbance force applied to the base platform and force generated by the actuator respectively. The desired displacement of the x_1 can be determined by converting and solving Eq. (1) in state-space form. The ratio of response of the mobile platform (x_1) to the displacement of the base platform (x_0) is called transmissibility (T).

$$\mathrm{T} = \left|\frac{x_1}{x_0}\right| = \sqrt{\frac{1+(2\xi p)^2}{(1-p^2)^2+(2\xi p)^2}} \quad (2)$$

where $\xi = c/2m_1\omega_n$=critical damping ratio, $p = \omega/\omega_n$, $\omega_n = \sqrt{k/m_1}$ = natural frequency.

The effectiveness of the isolator can be expressed in dB as:

$$\mathrm{E} = 10\log_{10}(1/\mathrm{T}) \quad (3)$$

The percentage effectiveness of the isolator can be expressed as:

$$\%\text{Isoaltion}=(1\text{-T})\times 100 \quad (4)$$

2.2 Principle of Active isolation

The goal of active vibration isolation is to diminish the vibration of a mechanism by automatic modification of the system's response. In the active isolation control the mechanism is instrumented with a set of actuators and sensors coupled with a controller. A model based control schemes like PD or Computed Torque Control

(CTC) methods may be used to update the active joint torques in every time second so that the platform deformations are negligible continuously. Movement and dynamic behavior of the mechanism are given in the task space. Here, the nonlinear dynamic equations of motion are reduced to linear form in terms of dynamic errors. Utilizing the computed torque control approach with a proportional-derivative (PD) outer control loop, the applied actuator torques are calculated at each time step using the following computed torque law.

$$\tau_a = M(q_a)(\ddot{q}_d + K_p e + K_d \dot{e}) + C(q_a, \dot{q}_a)\dot{q}_a \quad (5)$$

where *M* and *C* are the inertial and Coriolis matrices. $q_a, \dot{q}_a$ are the actual joint position and velocities. $\ddot{q}_d$ is the desired joint acceleration. τ_a is the computed torque applied to input links, K_p and K_d are the diagonal matrices of the proportional and derivative gains e and $\dot{e}$ are the vector of the position and velocity errors of the input links, $e = \mathrm{X}_d - \mathrm{X}_a$ and $\dot{e} = \dot{\mathrm{X}}_d - \dot{\mathrm{X}}_a$. The active vibration isolation scheme with CTC approach is shown in Fig. 3. Here, unlike external disturbance torques, here the base motion is considered in the kinematics itself.

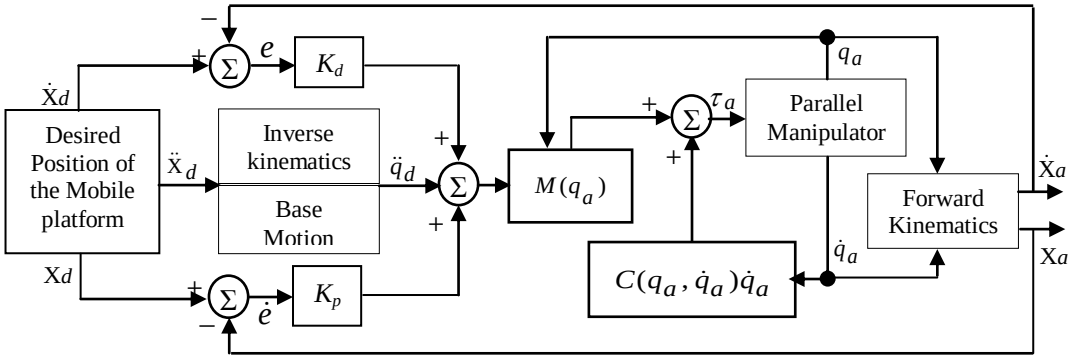

Figure 3: Active vibration isolation control scheme

3 Implementation of Isolator

A planar 3-RRR planar parallel platform is first modeled with the basic connector model forming the basis of the kinematic links and bodies. The planar 3-RRR parallel mechanism is modeled in SimMechanics which works under Simulink and illustrates a block diagram modeling environment where rigid bodies and their motions can be designed and simulated using the standard Newtonian dynamics. The modeled mechanism is shown in Fig. 4. The mechanism is modeled with eight bodies (base platform, mobile platform, six links) and nine revolute joints. Body-1 is considered as a base of the mechanism, it is connected between the ground and revolute joint-A_i (i=1,2,3) and the ground is connected with a customized joint to create the excitation to the base platform, also the ground is connected to the machine environment to to give the gravity direction. The base excitation in x and y directions of the base platform is recorded with a body sensor-1. The active link-*i* (i=1,2,3) is connected between the revolute joints A_i and B_i, passive link-*i* (i=4,5,6) is connected between the revolute joints B_i and C_i and the revolute joint A_i (i=1,2,3) is activated with joint actuators and the corresponding joint torque can be recorded

with joint sensor. Finally, all the C_i revolute joints are connected to the Body which is the mobile platform (end-effector) of the mechanism, using a body sensor at the center of the platform the response of the mobile platform can be recorded. It shows the motion transfer from first three active joints A_i to the mobile platform.

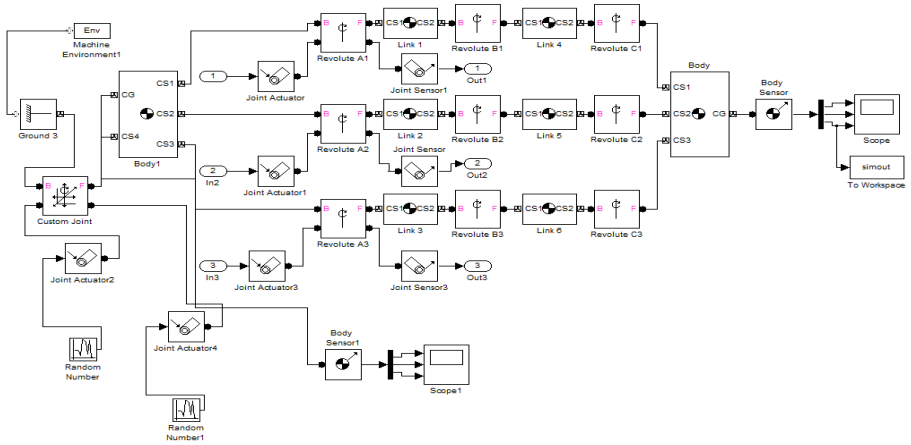

Figure 4: SimMechanics model of the mechanism

To create the model in ADAMS and SimMechanics the geometric and inertial parameters shown in Table 1 are used.

Table 1: Geometric and inertial properties of the mechanism

Link type	Length (mm)	Width (mm)	Mass (kg)	Moment of inertia (kg-mm^2)
Base platform	500	--	--	--
Active link	200	50	0.2	708.33
Distal link	200	50	0.2	708.33
Mobile platform	200	--	0.1	2000

The simulation results show the positioning capabilities of semi-active and active isolated mechanism under various external disturbances. The base platform is excited by a Gaussian distributed random signal as an input disturbance in x and y directions. Fig. 5 shows the displacement of the base in x and y directions with a mean zero and a variance 0.01.

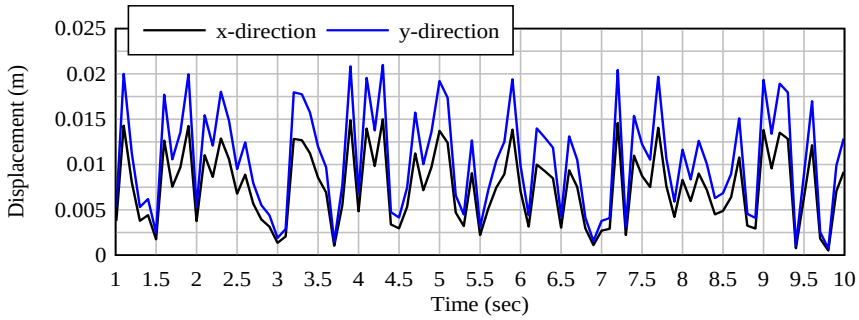

Figure 5: Base motion applied

A semi-active isolation with spring and damper at each active joint is modeled in Simulink as shown in Fig. 6 to evaluate the mechanism positioning capability

under semi-active isolation. The model is prepared as same as previous, in addition to that in semi-active isolation the spring and damper is considered at the active joint A_i (i=1,2,3) to suppress the base excitations. For the same base motions, the response of the mobile platform is shown in Fig. 7. After several trials the optimum stiffness and damping parameters considered are 100 N/m and 10Ns/m respectively, with these parameters the displacements at the mobile platform are reduced up to 40.48% in x-direction and 52.81% in y- direction.

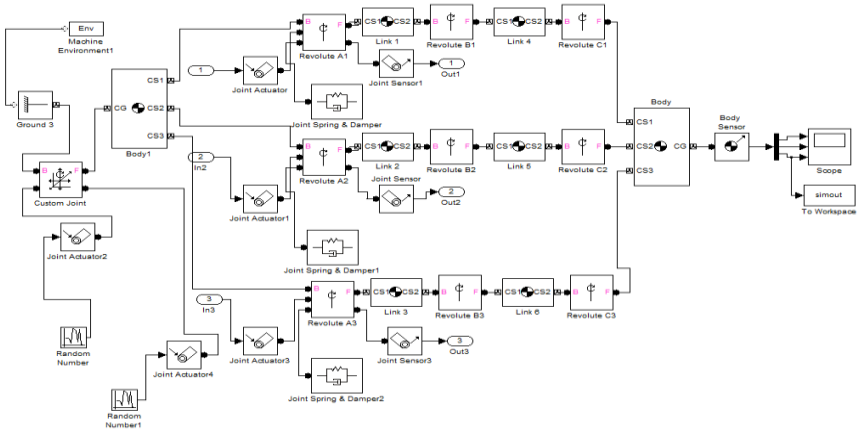

Figure 6: Semi-active isolation SimMechanics model

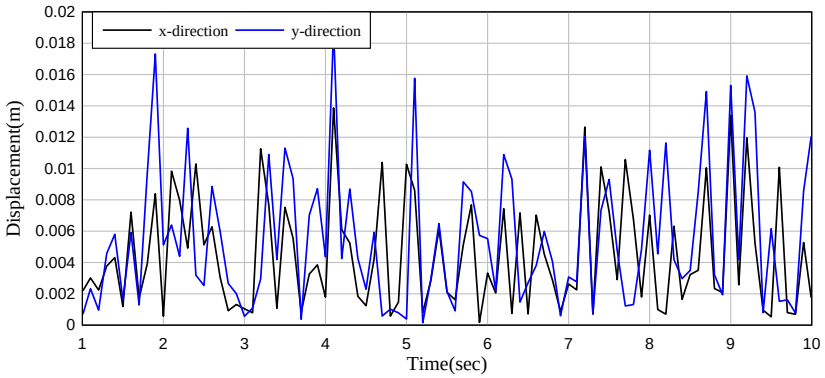

Figure 7: Mobile platform displacement histories with semi-active isolation

Fig.8 shows the dynamic response of the mobile platform under active control strategy. In this control the nonlinear dynamic differential equations are solved by a Runge-Kutta method and the optimum gain values are $K_p = 20$, $K_d = 2\sqrt{K_p}$. It is seen that the response of the mobile platform is reduced significantly under active control up to 57.22% in x-direction and 61.03% in y-direction and the corresponding actuated joint torques are shown in Fig. 9. At each instantaneous response of the mobile platform the corresponding actuated joint torques are provided. As the input disturbance is very small the control torques are also moderate.

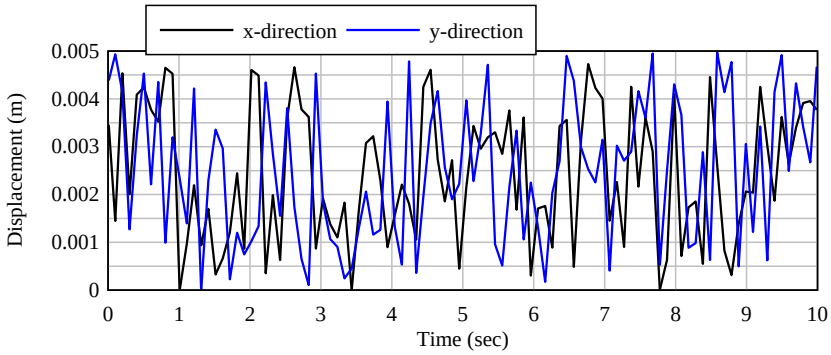

Figure 8: Mobile platform displacement histories with active isolation

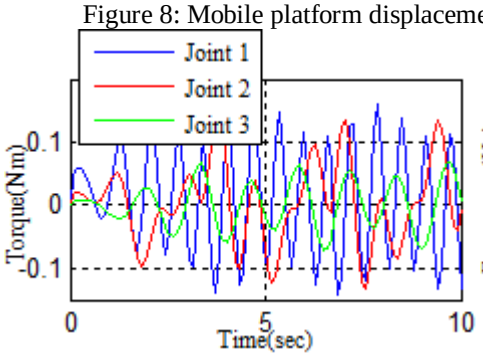

Figure 9: Actuated joint torques

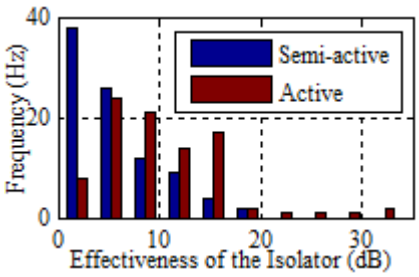

Figure 10: Effectiveness of the isolation control schemes

The mobile platform displacements due to active isolation control in x and y directions are much lower than those of semi-active isolation. Therefore, the significant improvement on vibration isolation performance is achieved by the active control. Even though the performance of the active isolation is better than the semi-active isolation, the improvement is only 14% in x-direction and 9% in y-direction. This may be due to the simple model based conventional CTC. In fact, there are many other uncertainties in the system such as external disturbances, parametric uncertainties. Therefore, the active vibration isolation for planar parallel mechanism with more robust control or intelligent tuning is required for the better performance of the mechanism.

Also, the effectiveness of the isolation is compared with semi-active and active control schemes. Here, the effectiveness in terms of displacement transmissibility is considered. Fig. 10 shows the effectiveness of the isolation schemes. From this, it is clearly observed that the maximum effectiveness of the semi-active and active isolation are 19.701 and 33.924 respectively, and also the frequency range of minimum effectiveness of semi-active is 81.5% more than the active isolation scheme. Therefore, the active isolation is more effective than semi-active isolation for the isolation of parallel mechanisms.

The mean transmissibility ratios and the percentage isolation in x and y directions for both the schemes are tabulated in Table 2. Here, we can observe that the minimum is the transmissibility ratio, maximum is the percentage isolation. In both x and y directions the percentage of isolation is maximum for the active control scheme only.

Table 2: Comparision of Semi-active and active isolation schemes

Method / Parameter	Semi-active		Active	
	x-direction	y-direction	x-direction	y-direction
Mean Transmissibility ratio	0.610	0.551	0.0023	0.0024
% Isolation	38.960	44.846	99.765	99.759

3.1 Experimental study

An experimental analysis is carried out to know further understanding of the motion transmission from mechanism. A scaled prototype of 3-RRR mechanism made out of rolled aluminium plates was fabricated and subjected to base excitation using a vibration shaker operated by a signal generator and power amplifier set-up as shown in Fig. 11. The test is carried-out by varying the frequency from 1-5000 Hz at constant input amplitude. The output of the mobile platform and base platform displacements are recorded in oscilloscope using two piezoelectric accelerometers and the frequency responses are obtained as shown in Fig.12. It is observed that even the mechanism is not controlled, there is some loss of motion from the base to mobile platform due to inherent damping in the linkage. Further, by accurately measuring the output at the mobile platform, the motors can be controlled appropriately to nullify the vibration levels at the mobile base.

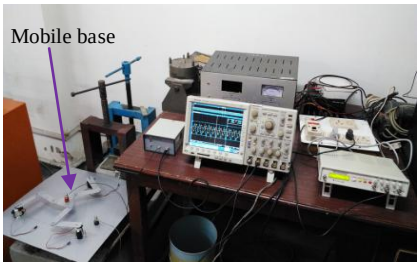

Figure 11: Experimental setup

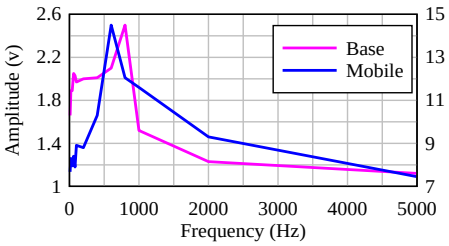

Figure 12: Frequency vs Amplitude at base and mobile platforms

4 Conclusions

In this paper, two scheme of control of planar 3-RRR parallel mechanism were proposed for vibration isolation of an instrument from base. In first case, an absorber mounted at each actuator joint reduces motion, while in second case an active mode using CTC controller was employed. The simulations results were presented for a test case and are very interesting. An experimental work was attempted to understand the further insights. It can be seen that the system achieves a good vibration isolation effect at the end-effector in x and y- directions.

References

[1] B. Li, W. Zhao, and Z. Deng, "Modeling and analysis of a multi-dimensional vibration isolator based on the parallel mechanism," Journal of Manufacturing. System, vol. 31 (1), pp. 50–58, 2012.
[2] Y. Yun and Y. Li, "A general dynamics and control model of a class of multi-DOF manipulators for active vibration control," Mechanism and Machine Theory, vol. 46 (10), pp. 1549–1574, 2011.
[3] Y. Cheng, G. Ren and S. Dai, "The multi-body system modelling of the Gough–Stewart platform for vibration control," Journal of Sound and Vibration, vol. 271(3–5), pp. 599–614, 2004.
[4] D. Kamesh, R. Pandiyan and A. Ghosal, "Passive vibration isolation of reaction wheel disturbances using a low frequency flexible space platform," Journal of Sound and Vibration, vol. 331 (6), pp. 1310–1330, 2012.
[5] R. A. Ibrahim, "Recent advances in nonlinear passive vibration isolators," Journal of Sound and Vibration, vol. 314 (3–5), pp. 371–452, 2008.
[6] W. Zhao, B. Li, P. Liu and K. Liu, "Semi-active control for a multi-dimensional vibration isolator with parallel mechanism," J. Vibration and Control, DOI. 1077546312439592, 2012.
[7] S. Chunsheng, Z. Zude and H. Yefa, "Semi-active mode fuzzy control for multi-dof floating raft isolation system with magnetic suspension isolators," Power and Energy Engineering Conference, Asia-Pacific, 2009, 1–5.
[8] M. Ahmadian and C. A. Pare, "A Quarter-Car Experimental Analysis of Alternative Semiactive Control Methods," Journal of Intelligent Material Systems and Structures, vol. 11 (8) , pp. 604-612, 2000.
[9] L. Kunquan and W. Rui, "Active Vibration Isolation of 6-RSS Parallel Mechanism Using Integrated Force Feedback Controllor," 3rd International Conference on Measuring Technology and Mechatronics Automation (ICMTMA), 2011, vol. 1, 314–317.
[10] A. Preumont, M. Horodinca, I. Romanescu, B. de Marneffe, M. Avraam, A. Deraemaeker, F. Bossens and A. Abu Hanieh, "A six-axis single-stage active vibration isolator based on Stewart platform," Journal of Sound and Vibration, vol. 300 (3–5), pp. 644–661, 2007.
[11] M. J. Brennan, M. J. Day and R. J. Randall, "Experimental investigation into the semi-active and active control of longitudinal vibrations in a large tie-rod structure," Journal of Vibration and Acoustics, Transactions of the ASME, v 120 (1), pp. 1-12, 1998.
[12] G. Z. Yao, F. F. Yap, G. Chen, W. H. Li and S.H. Yeo, "MR damper and its application for semi-active control of vehicle suspension system," Mechatronics, vol. 12, pp. 963-973.2002.
[13] T. Yang, J. Ma, Z-G. Hou and M. Tan, "Robust back stepping control of active vibration isolation using a Stewart platform," IEEE International Conference on Robotics and Automation, Kobe, 2009, 1788-1793
[14] I. M. Buzurovic and D. L. Debeljkovic, "Robust control for parallel robotic platforms," IEEE 16th International Conference on Intelligent Engineering Systems (INES), Lisbon, 2012, 45-50.
[15] Y. Wu, K. Yu, J. Jiao and R. Zhao, "Dynamic modeling and robust nonlinear control of a six-DOF active micro-vibration isolation manipulator with parameter uncertainties," Mechanism and Machine Theory, vol. 92, pp. 407–435, 2015.